

## Deciphering Excited State Evolution in Halorhodopsin with Stimulated Emission Pumping

Oshrat Bismuth,<sup>†</sup> Pavel Komm,<sup>†</sup> Noga Friedman,<sup>‡</sup> Tamar Eliash,<sup>‡</sup> Mordechai Sheves,<sup>\*,‡</sup> and Sanford Ruhman<sup>\*,†</sup>*Institute of Chemistry and the Farkas Center for Light Induced Processes, The Hebrew University, Jerusalem 91904, Israel, and Department of Organic Chemistry, The Weizmann Institute of Science, Rehovot 76100, Israel**Received: November 15, 2009; Revised Manuscript Received: January 15, 2010*

The primary photochemical dynamics of *Hb. pharaonis* Halorhodopsin (pHR) are investigated by femtosecond visible pump–near IR dump–hyperspectral probe spectroscopy. The efficiency of excited state depletion is deduced from transient changes in absorption, recorded with and without stimulated emission pumping (SEP), as a function of the dump delay. The concomitant reduction of photocycle population is assessed by probing the “K” intermediate difference spectrum. Results show that the cross section for stimulating emission is nearly constant throughout the fluorescent state lifetime. Probing “K” demonstrates that dumping produces a proportionate reduction in photocycle yields. We conclude that, despite its nonexponential internal conversion (IC) kinetics, the fluorescent state in pHR constitutes a single intermediate in the photocycle. This contrasts with conclusions drawn from the study of primary events in the related chloride pump from *Hb. salinarum* (sHR), believed to produce the “K” intermediate from a distinct short-lived subpopulation in the excited state. Our discoveries concerning internal conversion dynamics in pHR are discussed in light of recent expectations for similar excited state dynamics in both proteins.

## Introduction

Halorhodopsin (HR) is a member of the retinal protein (RP) family active in Halophilic archaea, and serves as an inward directed chloride pump. Its function is energized by photoisomerization of a retinal chromophore covalently bound to a lysine residue to form a protonated Schiff base (PSB) linkage. This function is achieved in a cyclic transformation which begins with light absorption and within milliseconds leads to reconstitution of the protein with translocation of a single halide ion. Various analogues of HR have been discovered, but the most studied pigments are from *Halobacterium salinarum* (sHR)<sup>1</sup> and *Natronomonas pharaonis* (pHR).<sup>2</sup> An important difference between sHR and pHR is the ratio between *trans* and *cis* retinal isomers. In the dark adapted form of sHR, 45% of the protein is all-*trans*, while the percentage increases to 75% following light adaptation. In pHR, however, the all-*trans* percentage (85%) is unchanged in the dark and light forms.<sup>3</sup> In contrast to sHR, the 13-*cis* pigment does not have a detectable photocycle<sup>4</sup> which simplifies kinetic study of the all-*trans* form.

The amino acid sequence of HR was determined and has revealed considerable similarity to bacteriorhodopsin (BR).<sup>5,6</sup> In keeping with the lack of proton pumping activity of HR, sequence alterations were found in crucial residues. HR is lacking the equivalent of Asp85 which serves as the PSB proton acceptor in the BR photocycle. This residue is replaced in both pHR and sHR by Thr which is part of the chloride binding site. In BR, Asp96 is the proton donor to the Schiff base (SB) in the second half of the photocycle and is substituted by Ala in HR. The chloride is bound in the vicinity of the SB as detected by resonance Raman spectroscopy,<sup>7</sup> and x-ray diffraction studies

indicate that it is part of the PSB counterion, substituting the role played by Asp85 in BR.<sup>8</sup>

As in all archaeal rhodopsins, internal conversion (IC) and all-*trans* to 13-*cis* photoisomerization of the embedded retinal moiety take place within a few picoseconds.<sup>9</sup> Despite its briefness, this stage holds the key to storing the photon energy necessary for the Cl<sup>−</sup> transport across the cell membrane. To understand how this is accomplished, femtosecond pump–probe spectroscopy was recently employed to record primary events unleashed in pHR upon light absorption.<sup>10</sup> The dependence of pHR\* dynamics on the substitution of Cl<sup>−</sup> with other halide ions was also tested. In the native chloride environment, kinetics of pHR internal conversion, following a 50 fs initial phase of spectral shifting, were well fit to a biexponential decay function with time constants of ~1.5 and ~4 ps, both with nearly equal amplitudes. Substituting chloride with heavier halide ions mildly slowed this process down, and also altered the relative amplitudes of the decay components.

Interpretation of these results was based on earlier studies of sHR.<sup>11,12</sup> Ultrafast investigation of primary events in sHR also exhibited biexponential picosecond IC kinetics with slightly longer decay times (~1.5 and ~8.5 ps). In combination with the uncharacteristically low quantum yield (~30%) for isomerization in this pigment, the biexponential IC in sHR was assigned to two distinct excited state populations, only one of which is a photocycle intermediate, the other leading back to the reactant state. Subsequent femtosecond visible pump–mid-IR–probe experiments on sHR assigned the shorter of these decays (1.5 ps) to the reactive channel by demonstrating that the photoproducts appear on a similar time scale.<sup>13</sup> In view of the functional similarities of both proteins, the same reactive scenario was adopted for interpreting primary events in pHR as well.<sup>10</sup>

Verifying this assignment is important on a number of levels. First, while biexponential IC kinetics with similar time scales

\* Corresponding authors.

<sup>†</sup> The Hebrew University.

<sup>‡</sup> The Weizmann Institute of Science.

are observed in both halorhodopsins, assuming that fine dynamic details of primary events in both chloride pumps are the same should be alternatively examined. The prevalence of biexponential IC kinetics in most archaeal retinal proteins, and in retinal protonated Schiff base (RPSB) in solution,<sup>14–18</sup> makes a ruling on this issue most important. In the case of RPSB in solution, very similar excited state decay kinetics has been assigned by some to cooling of a single reactive  $S_1$  population during the process of IC. In other studies, the biexponential  $S_1$  decay has been suggested to stem from separate excited state populations akin to the scenario assigned to sHR. Biexponential IC kinetics is so widespread in bacterial retinal proteins that a theoretical study dedicated solely to this issue presents excited state potential topologies which can reproduce similar dynamics.<sup>19</sup> This ubiquity makes the determination of a correct dynamic scenario for primary events in this representative natural pigment all the more interesting and significant. Finally, though quantum yields of retinal protein photocycles are at most  $\sim 65\%$ , nearly all transient spectral signatures of their primary events have been assigned to reactive fluxes, unlike the long fluorescent population in HR.

In order to address this question, we have employed a method previously used to probe fluorescent state evolution in bacteriorhodopsin (BR).<sup>20</sup> It involves a three pulse pump/dump/probe sequence. The pump serves to initiate photoexcitation in the characteristic mid visible  $S_0$ – $S_1$  absorption band, peaking at 575 nm. At a controlled delay, an intense near-infrared (NIR) dump pulse centered at  $1.15\ \mu\text{m}$  is introduced to stimulate emission back down to  $S_0$ . As in the case of BR, the fluorescent state in HR has characteristic absorption and stimulated emission bands in the NIR which overlap until  $\sim 900\ \text{nm}$ , with emission alone extending to longer wavelengths.<sup>21</sup> Accordingly, the NIR dump wavelength is chosen to induce only emission and to avoid simultaneous excitation from  $S_1$  to  $S_n$ . The dump's impact on the fluorescent state population is recorded by probing in the stimulated emission band, while its effect on the photocycle is investigated by probing the difference spectrum of the metastable ground state product "K".

In the present experiment, the effects of both pump and dump are followed by recording changes in optical density of the sample from 450 to 950 nm as a function of time, starting from the initial pump interaction and ending with the completion of internal conversion and generation of the first relaxed photocycle intermediate "K". Hyperspectral probing employed here allows coverage of both the stimulated emission and the "K" absorption bands. This improvement upon the previous experiment allows verification that the dump does not induce transitions aside from the desired emission and that only the "K" intermediate is generated following decay of  $S_1$ . This is repeated with and without dump pulses, and for different pump–dump delays throughout the  $S_1$  lifetime.

The experiments described below show that as in BR, aside from a very brief initial stage of spectral evolution, the cross section for NIR dumping is conserved for the duration of the  $S_1$  lifetime.

The dumping also depletes the generation of "K" to a degree which is commensurate with the dump induced depletion. These results show that, contrary to the behavior reported for sHR, no obvious difference can be detected between the excited population before and after culmination of the rapid initial stage of IC (1.5 ps), either in terms of the cross section for stimulating emission in the NIR or in terms of the effect of that dumping on the generation of later photocycle products.

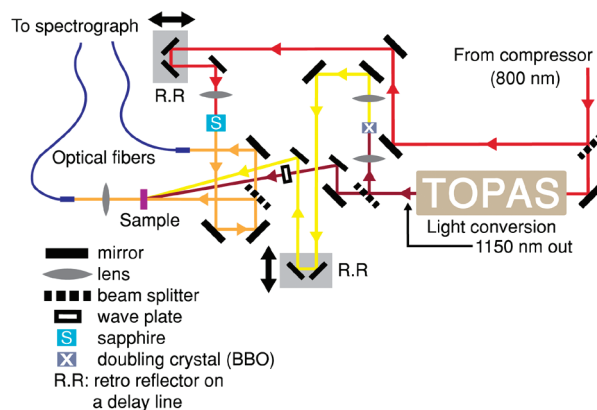


Figure 1. Experimental setup.

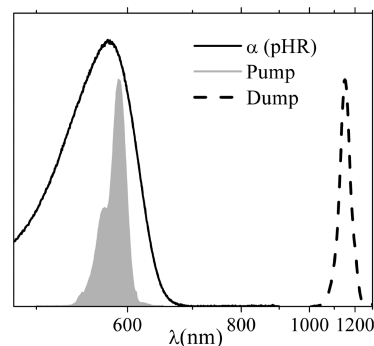
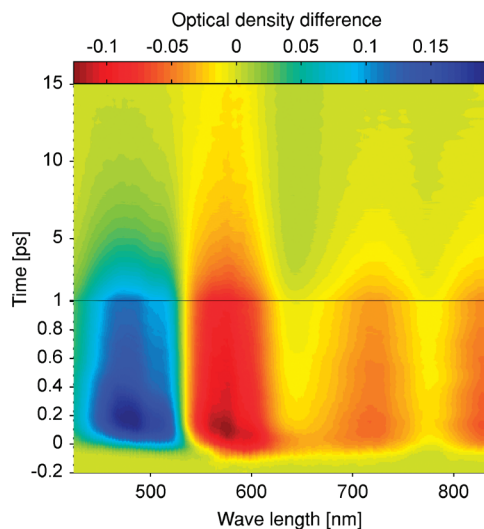


Figure 2. Normalized absorption spectra of pHR together with normalized intensity spectra of pump and dump pulses used in this study.

## Experimental Methods

pHR samples were prepared similarly to the method previously described<sup>22</sup> with some modifications. Transformed *E. coli* BL21 cells were grown at 37 °C in LB medium with 50 mg/mL kanamycin in a 10 L fermentor. At an  $\text{OD}_{600}$  of  $\sim 1$ , 0.5 mM IPTG and 10  $\mu\text{M}$  all-*trans* retinal were added. After an induction period of 4 h, the cells were harvested and stored at  $-20\ ^\circ\text{C}$ . The cells were thawed, suspended in a Tris–HCl buffer, pH 7, and centrifuged. The pellet was solubilized in buffer S (0.5% DM, 500 mM NaCl, 50 mM MES, 5 mM imidazole, pH 6.0) and stirred overnight at 4 °C. After centrifugation, the supernatant was run through a Ni-NTA agarose column at 4 °C. The Ni-NTA resin was washed extensively with buffer W (0.06% DM, 500 mM NaCl, 50 mM MES, 5 mM imidazole, pH 6.0), increasing the imidazole concentration (up to 100 mM) to remove nonspecifically bound proteins. Subsequently, pHR was eluted in buffer E (0.06% DM, 500 mM NaCl, 50 mM Tris–HCl, 300 mM imidazole, pH 7.8) and transferred to the final buffer (0.06% DM, 300 mM NaCl, 50 mM Tris–HCl, pH 7) using an Amicon centrifugal filter (cutoff, 10 K).

Laser pulses were derived from a homemade multipass Ti: sapphire amplifier, producing 30 fs pulses centered at 790 nm, with an energy of  $\sim 0.5\ \text{mJ}$ , operated at 450 Hz (see the system schematic in Figure 1). 50% of the output was used to pump a parametric amplifier (TOPAS, Light Conversion), generating signal pulses at  $1.15\ \mu\text{m}$ . These were split into two arms, one generating pump pulses at 580 nm by frequency doubling in 0.25 mm of BBO. The other arm provided dump pulses in the NIR (see spectra in Figure 2). A multifilament supercontinuum was generated by focusing  $\sim 2\ \mu\text{J}$  of the 800 nm fundamental in a 2.5 mm sapphire plate, and split to produce probe and reference beams.



**Figure 3.** Contour map of transient difference spectra corrected for probe group delay dispersion from  $-0.2$  to  $15$  ps, shown on a split time axis with an expanded scale up to  $1$  ps.

Pump, probe, and dump pulses, all polarized identically, were focused into a  $0.5$  mm flow cell equipped with  $0.15$  mm crown-glass windows. Probe pulses were focused to a spot of  $0.1$  mm, with pump and dump beam diameters at least twice that. The pump flux was estimated from the optical density of the  $S_1$  bleach in the data (Figure 3, at  $580$  nm) to be  $\sim 6.5 \times 10^{14}$  photons/cm<sup>2</sup>, and the linearity of the signal with pump intensity up to this value was verified. As for the dump pulse flux, it is estimated to be  $\sim 5 \times 10^{15}$  photons/cm<sup>2</sup>. An accurate measurement of the fluence for this beam was limited by sensitivity of the detector used, and its large beam waist in comparison with the other pulses. The dump alone was shown to have no detectable influence on the sample. The sample was continuously syringe pumped through the cell at a rate which ensured replenishment between excitations. Probe and reference pulses were directed through fibers to a double diode array spectrograph setup. The two registered spectra from pulse pairs provide a  $512$  pixel absorption spectrum. Such spectra were taken with and without pump for consecutive pulse pairs. Subtraction of these provided the  $\Delta OD$  spectra which are averaged to produce the presented data. The relative timing of all three pulses is controlled by automated delay lines. Global fitting of time corrected transient  $\Delta OD$  to decay associated spectra (DAS) was conducted with a labview-based software package written in house and based on standard methods.<sup>23</sup>

## Results

Transient time corrected spectra were collected with parallel polarization of pump and probe in view of the relatively weak intensity of the  $HR_{580} - K_{640}$  difference spectrum. Figure 3 presents a color graded contour map obtained without applying the IR dumping pulse, which serves as a reference for the dumping experiments. Since no hyperspectral pump–probe data from pHR have been published, its brief description is provided herewith. The blue side of the spectrum is dominated by the  $S_1$  absorption band centered at  $475$  nm, exhibiting a very brief blue shift at early times. This band partially overlaps the strong excess transmission induced by  $S_0$  bleaching. On the red side of the ground state bleach, a double humped stimulated emission band rises upon excitation. All of these features decay within  $\sim 20$  ps, leaving the stable “K” intermediate difference spectrum which reflects the mild red shift in this species absorption band

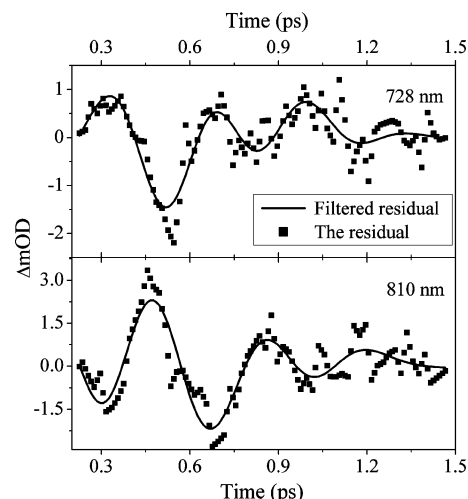


**Figure 4.** Oscillatory residuals obtained after the subtraction of kinetic fits to the data at two probing wavelengths above and below the excited state emission, along with curves obtained after high frequency noise filtering.

relative to that of the ground state. The transient difference spectra in Figure 3, including the double peaked emission band, resemble the published hyperspectral pump probe data obtained from the related sHR chloride pump.<sup>21</sup> As in other retinal proteins and retinal protonated Schiff base, the double peaked shape is attributed to overlapping emission and absorption bands in  $S_1$ .<sup>24</sup>

Close examination of the excited state's stimulated emission band in Figure 3 reveals a modulation pattern consistent with coherently excited low frequency  $S_1$  vibrations akin to those reported for BR and RPSB in solution with characteristic frequencies of  $170$  and  $120$  cm<sup>−1</sup>, respectively.<sup>25</sup> Fourier analysis of residuals obtained after subtraction of kinetic fits to transients in the red part of the spectrum produced a central frequency lying below both of those cited above. Assigned to torsional motions involving large portions of the molecular backbone,<sup>26</sup> the derived frequency for pHR is almost twice as slow as in BR. It modulates the absorption around  $730$  and  $810$  nm at a frequency of only  $\sim 90$  cm<sup>−1</sup>, as can be seen in Figure 4. The smooth lines superimposed on the residuals are obtained by high frequency noise filtering. The undulations change sign when going from  $730$  to  $810$  nm, two wavelengths which bracket both the spontaneous emission and absorption bands of the fluorescent state of pHR from below and above, respectively, and thus may involve both transitions. Nonetheless, the recent observation of similar modulations in the fluorescence of RPSB in solution strengthens the expectation that this signature relates primarily to emission.<sup>27</sup>

After reduction of the raw data by singular value decomposition (SVD),<sup>28</sup> the transient spectra are characterized by global fitting to a parallel kinetic scheme, including convolution with a Gaussian instrument response function of  $70$  fs fwhm. This analysis produces a series of decay associated spectra, each assigned an exponential time constant. In order to achieve reconstruction of the experimental data, it was necessary to model its temporal behavior using five decay components with associated decay times of  $0.0$  ( $\delta$  function),  $0.22 \pm 0.02$ ,  $2.0 \pm 0.2$ ,  $5.0 \pm 0.5$ , and  $\infty$  ps. Figure 5 depicts the resulting spectra. The three finite decay time associated spectra are nearly the same at the blue and red edges of the map but deviate in the region of reactant and photoproduct absorption.

Dump pulses polarized parallel to the pump and probe were introduced in two different experiments. The goal of the first



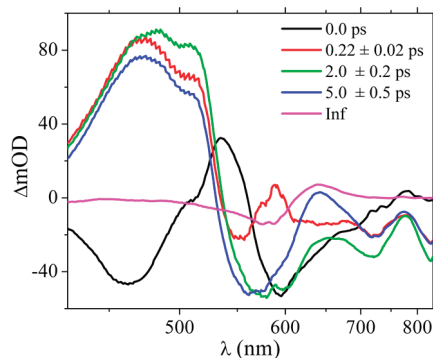


**Figure 5.** Decay associated spectra (DAS) derived by global fitting of the data to a multiexponential functional with the depicted decay constants.

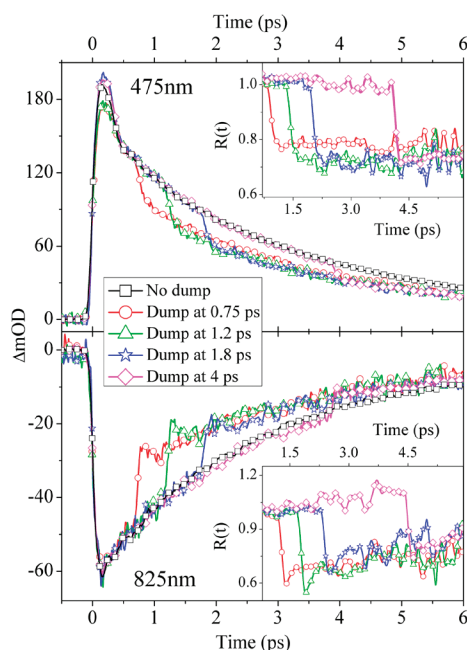


**Figure 6.** Pump-dump-probe data presented at two probing wavelengths and various dumping delays with identical dump fluences. For reference, a scan taken without dump is included as well. The ratio of transient signal with dump to that without is presented in the insets for the data in the main figure.

was to investigate the effect of dumping on the excited state population, and how this depends on pump-dump delay. The second was intended to test whether, and to what extent, the stimulated emission pumping at different times changes the population of the photocycle, as reflected by dump induced changes in the absorption of  $K_{640}$  after IC is complete at 30 ps. Figure 6 summarizes the outcome of the initial experiment. The dumping data from the excited state's absorption and emission bands (averages from 470–480 nm and 823–833 nm, respectively) is shown along with the corresponding averaged portions of the reference spectrum. The insets present ratios of the transients with and without IR irradiation. Immediately perceptible is the convergence of the post dump portions of the transients for SEP delays  $\geq 0.75$  ps within the noise margins regardless of the dump timing. One earlier dumping delay results in a slightly lower ultimate depletion. Finer scrutiny reveals differences in SEP induced changes in emission and absorption bands immediately after the dump. The former exhibits an excess depletion of emission which recovers within a few hundred femtoseconds. In contrast, an opposite and milder trend is apparent in the blue absorption band where there is a delayed

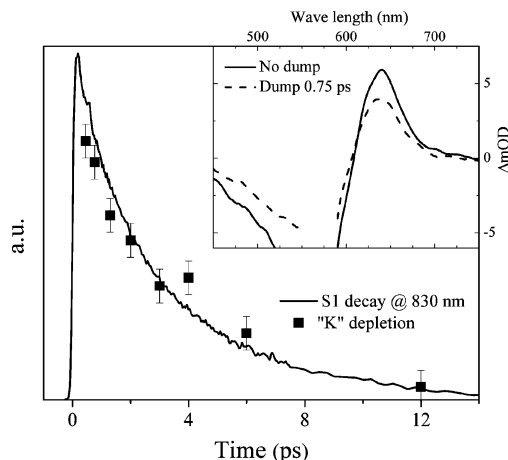


**Figure 7.** The fractional reduction in the generation of “K” as a function of the dump delay along with a stimulated emission scan representing the instantaneous concentration of excited states on the same time scale. Inset: difference spectra at 30 ps showing the effect of dumping at 0.75 ps on photoproduct generation.

component of absorption depletion which recedes again within  $\sim 300$  fs. These features will be discussed in detail below.

The independence of  $S_1$  depletion probability on the dump delay in BR was assigned to invariance of the emitting excited protein population during the lifetime of the fluorescent state.<sup>20</sup> As in that study, here also that interpretation is corroborated by testing the ultimate effect of dumping on photocycle population by measuring the absorption of  $K_{640}$ . Difference spectra of the relaxed photoproduct were measured at a delay time of 30 ps. The nondecaying DAS in Figure 5 is a good example of their appearance. For eight SEP delays spanning the fluorescence lifetime, the fractional reduction in the K's difference spectrum was measured, and results are plotted in Figure 7 which compares the magnitude of this measure with the decay of excited state stimulated emission at 830 nm. The inset presents “K” difference spectra with and without dump pulses for the shortest dump delay for comparison. Results show the photocycle can be short-circuited throughout the  $S_1$  lifetime, with an efficiency which matches the instantaneous concentration of excited proteins within experimental error.

## Discussion

Hyperspectral transient absorption data in Figure 3 resemble those published a decade ago for sHR,<sup>21</sup> including relative amplitudes of the various bands, and the double humped appearance of the emission band assigned to an overlapping excited state absorption band. As stated above, the decay times obtained from fitting are somewhat faster for pHR, and are in agreement with the recent study of Nakamura et al. One aspect of our data was not observed there, and involves the very prompt nonexponential decay ( $\sim 200$  fs) observed in the blue excited state absorption band at  $\sim 490$  nm. Since the samples are equivalent, this difference probably involve particulars of the pump interaction.

The high pump fluence and large resulting  $\Delta OD$  were resorted to so that small differences in concentrations of “K”, the first relaxed ground state intermediate in the photocycle, could be measured with sufficient precision. The relatively faint  $HR_{580} - K_{640}$  difference spectrum makes the essential observation of small changes in this yield challenging. The possibility that this rapid decay peculiar to our data stems from high pump intensities was ruled out by verifying that the transient signals

at  $\sim 500$  nm are unchanged over a broad range of pump intensities. It is likely that this difference is the result of shorter pump wavelengths employed here, but this sole conflict with the earlier study will require further investigation. In any case, SEP experiments only involve dumping after this phase of evolution, and perfect agreement of our  $\Delta OD$  data with previous results beyond that phase allows for direct comparison, both of the data and its interpretation.

In earlier studies of sHR, the assignment of reactivity to the fast phase of IC was based on the rapid appearance of absorption near 650 nm where the K difference spectrum peaks, an appearance which is much faster than the overall relaxation back to the ground state.<sup>11</sup> It is interesting therefore to examine this aspect of this data obtained for pHR. Differences between the three exponentially decaying DAS tell the story in this regard. While the DAS decaying in 2 ps exhibits significant negative amplitude at 640 nm, that associated with the slower decay is virtually zero around that wavelength. Thus, as in sHR, the pump–probe data exhibit a rise at the peak of the HR – K spectrum which takes place much faster than the total course of IC. Accordingly, using the same arguments as in refs 11 and 12, the ultrafast transient absorption spectra in pHR could equally be interpreted in terms of one fast and reactive density in  $S_1$ , along with a slower nonproductive population in the excited state. This finding is in line with the assumption that pHR and sHR undergo similar photochemistry but contradicts the results of experiments described here. We will return to this point below.

The reduced frequency of modulations excited in the fluorescent state relative to other RPs and RPSB in solution is interesting. In a previous study, the increased frequency of torsional coherences detected in BR relative to RPSB was assigned to increased rigidity of the retinal conformation due to the protein surroundings. In analogy, one would thus conclude that insertion into the apoprotein of HR actually softens the torsional potential relative to RPSB in solution. It is noteworthy that a recent simulation of dynamics in HR has suggested that in “K” the potential governing the torsion around the  $C_{13}=C_{14}$  bond is in fact much flatter than in the ground state.<sup>29</sup> The question of whether this carries over also to the excited state is not directly addressed and will require more study.

Having characterized the spectral evolution of excited pHR, the underlying dynamics are tested by probing how the transient spectra are altered by introducing a NIR dump pulse, and how this depends on the pump–dump delay. From  $R(t) = [\Delta OD_{\text{dump}} / \Delta OD_{\text{no dump}}](t)$  in the insets to Figure 6, it is obvious that throughout the excited state lifetime it can be depleted by the dump pulses at 1.16  $\mu\text{m}$ . This is apparent in the excited state absorption and throughout the NIR emission band as well. Furthermore, transients in both ranges demonstrate that the fraction of OD depleted is independent of the dump delay, since  $R(t)$  asymptotically approaches the same value regardless of the dump delay. The delays tested are spread over a range during which more than 90% of the excited molecules repopulates  $S_0$  through IC.

One trend of  $R(t)$  which is wavelength dependent is the initial excess bleach which is detected in the stimulated emission band, and decays within a few hundred femtoseconds to the asymptotic limit. A similar feature was reported in a number of other pump/dump/probe experiments conducted with high time resolution in large organic molecules.<sup>20,30</sup> A comparison of the insets to the upper and lower panels of Figure 6 shows that while this excess bleach is prominent in stimulated emission ( $\lambda > 700$  nm), a weaker opposite trend is observed in  $S_1$  absorption (450–500

nm). The former has been assigned to impulsively generated wave packets on the state to which dumping or repumping takes place, and/or to the buildup of localized “holes” in  $S_1$ . Both can involve intra- and intermolecular coordinates. The decay is accordingly assigned to dephasing or dispersal of both.

The appearance of excess bleach when probing in the dump transition makes perfect sense, since the resulting  $S_0$  wave packets and the holes burned in  $S_1$  both specifically reduce stimulated emission near the dumping wavelength. Their effect on transition from  $S_1$  to higher surfaces depends on the potential minima displacements between the coupled surfaces. In any case, a localized depletion in  $S_1$  should influence both transitions, but emission alone involves dynamics in the ground state to which the population is dumped. The difference in sign of these signatures when probing in emission and absorption from  $S_1$  must reflect significant differences in geometry and/or charge distribution between  $S_0$  and the  $S_n$  involved. This information should prove valuable for mapping the electronic states involved both in the photochemistry and spectroscopy of retinal proteins.<sup>31</sup>

Invariance over time of the  $S_1$  cross section for emission already suggests that its spectral features belong to a single effective excited state population. It is unlikely that two distinct excited populations would respond identically to a stimulating NIR field. However, this is indirect evidence. It is verified by the changes in the generated “K” population with and without dumping. The results portrayed in Figure 7 demonstrate not only that the dumped population circumvents the photocycle but that this can be achieved at all stages of  $S_1$  lifetime, to a degree which is proportional to the residual concentration of excited molecules. As in BR, the fact that the dumped population is excluded from biological activity teaches us more than the fact that all stages of IC can lead to isomerization. It also shows that fluorescence takes place from an excited configuration far from the curve crossing which facilitates IC to the ground state. In the study of BR, this was suggested to reflect a barrier in the excited state between the relaxed fluorescent state and the reactive channel toward the seam for crossing to the ground state enabling the isomerization to take place, a scenario evoked for explaining the pump–probe data on pHR as well.<sup>10</sup>

How can this be reconciled with the finding, as in sHR, that the rise in OD @ 650 nm, the peak of the “K” difference absorption spectrum, takes place within  $\sim 2$  ps? A clue to answering this may be found in a study of primary events in an artificial BR pigment where the prosthetic group is substituted with a retinal molecule whose  $C_{13}=C_{14}$  bond is locked in the *trans* configuration by its inclusion in a five-membered ring structure.<sup>32,33</sup> While the buildup of a fluorescent state akin to that in BR was prompt, internal conversion back to the initial conformation was shown to take nearly 40 times longer in the locked pigment, proving that the 0.5 ps decay to “J” coincides with the stage of bond twisting. Another finding, pertinent to our current riddle, was that, despite the frustration of “K” formation, a rapid buildup of excess absorbance at 650 nm was observed in locked BR as well. This proves that dynamic changes in  $S_1$  other than formation of an isomerized ground state molecule can produce this response, making its interpretation ambiguous. In fact, the experimental strategy used here was devised specifically to test earlier interpretations with a method which relies on more direct evidence. Accordingly we attach more credence to the stimulated emission results in interpreting the source of IC dynamics.

We conclude that neither the nonexponential IC kinetics nor the fast rise of absorption at 640 nm reflect a fast reactive and slower back reactive population in the case of pHR. This is not

to say that no back reaction occurs—after all a 0.5 quantum efficiency in Hb. *Pharaonis* has been reported.<sup>34</sup> However, this back reaction can take place as bifurcation at the crossing back to the ground state as portrayed in most proposed schemes. As in BR, the fluorescent state must represent a single photocycle intermediate, with the nonexponential aspects of its decay stemming from other dynamic excited state processes such as vibrational relaxation, etc. Clearly, this conclusion does not necessarily carry over to the related sHR which might undergo significantly different photochemistry. It is sHR and not pHR which has been probed with ultrafast mid-IR pulses and shown to exhibit a buildup of products for only a fraction of the fluorescent state lifetime. Nonetheless, our expanding experience with these closely related proteins may equally indicate that these trends carry over to many archaeal rhodopsins, and that parallel excited state dynamics are not a general feature of RP photochemistry after all. Deciding this could be aided significantly by a complementary study of pHR in the mid-IR, or alternatively by a study akin to that reported here on the excited state dynamics of HR active in *H. salinarum*.

**Acknowledgment.** This work was supported by the Israel Science Foundation (ISF) which is administered by the Israel Academy of Sciences and the Humanities, the US-Israeli binational science foundation, and the Kimmelman center for Biomolecular Structure and Assembly (to M.S.). The Farkas Center is supported by the Minerva Gesellschaft, GmbH, Munich, Germany. M.S. holds the Katzir-Makineni chair in chemistry.

## References and Notes

- (1) Lanyi, J. K. *Annu. Rev. Biophys. Chem.* **1986**, *15*, 11–28. Havelka, W. A.; Henderson, R.; Heymann, J. A. W.; Oesterhelt, D. *J. Mol. Biol.* **1993**, *234*, 837–846.
- (2) Bivin, D. B.; Stoekenius, W. *J. Gen. Microbiol.* **1986**, *132*, 2167–2177.
- (3) Zimanyi, L.; Lanyi, J. *J. Phys. Chem. B* **1997**, *101*, 1930–1933.
- (4) Varo, G.; Brown, L. S.; Sasaki, J.; Kandori, H.; Maeda, A.; Needleman, R.; Lanyi, J. K. *Biochemistry* **1995**, *34*, 14490–14499.
- (5) Blanck, A.; Oesterhelt, D. *EMBO J.* **1987**, *6* (1), 265–273.
- (6) Mukohata, Y.; Ihara, K.; Tamura, T.; Sugiyama, Y. *J. Biochem.* **1999**, *125* (4), 649–657.
- (7) Gersher, S.; Mylrajan, M.; Hildebrandt, P.; Baron, M. H.; Müller, R.; Engelhard, M. *Biochemistry* **1997**, *36*, 11012–11020.
- (8) Kolbe, M.; Besir, H.; Essen, L. O.; Oesterhelt, D. *Science* **2000**, *288*, 1390–1396.

- (9) Diller, R. In *Ultrashort Laser Pulses in Biology and Medicine*; Braun, M., Gilch, P., Zinth, W., Eds.; Springer: Berlin Heidelberg, 2008.
- (10) Nakamura, T.; Takeuchi, S.; Shibata, M.; Demura, M.; Kandori, H.; Tahara, T. *J. Phys. Chem. B* **2008**, *112*, 12795–12800.
- (11) Kandori, H.; Yoshihara, K.; Tomioka, H.; Sasabe, H. *J. Phys. Chem.* **1992**, *96*, 6066–6071.
- (12) Arlt, T.; Schmidt, S.; Zinth, W.; Haupts, U.; Oesterhelt, D. *Chem. Phys. Lett.* **1995**, *241*, 559–565.
- (13) Peters, F.; Herbst, J.; Tittor, J.; Oesterhelt, D.; Diller, R. *Chem. Phys.* **2006**, *323*, 109–116.
- (14) Kandori, H.; Sasabe, H. *Chem. Phys. Lett.* **1993**, *216*, 126–172.
- (15) Hamm, P.; Zurek, M.; Roschinger, T.; Patzelt, H.; Oesterhelt, D.; Zinth, W. *Chem. Phys. Lett.* **1996**, *263*, 613–621.
- (16) Hamm, P.; Zurek, M.; Roschinger, T.; Patzelt, H.; Oesterhelt, D.; Zinth, W. *Chem. Phys. Lett.* **1997**, *268*, 180–186.
- (17) Hou, B.; Friedman, N.; Ruhman, S.; Sheves, M.; Ottolenghi, M. *J. Phys. Chem. B* **2001**, *105*, 7042–7048.
- (18) Zgrablic, G.; Voitchovsky, K.; Kindermann, M.; Haacke, S.; Chergui, M. *Biophys. J.* **2005**, *88*, 2779–2788.
- (19) Olivucci, M.; Lami, A.; Santoro, F. *Angew. Chem., Int. Ed.* **2005**, *44*, 5118–5121.
- (20) Ruhman, S.; Hou, B.; Friedman, N.; Ottolenghi, M.; Sheves, M. *J. Am. Chem. Soc.* **2002**, *124*, 8854–8858.
- (21) Kobayashi, T.; Kim, M.; Taiji, M.; Iwasa, T.; Nakagawa, M.; Tsuda, M. *J. Phys. Chem. B* **1998**, *102*, 272–280.
- (22) Hohenfeld, I. P.; Wegener, A. A.; Engelhard, M. *FEBS Lett.* **1999**, *442*, 198–202.
- (23) van Stokkum, I. H. M.; Larsen, D. S.; van Grondelle, R. *Biochim. Biophys. Acta* **2004**, *1658*, 262.
- (24) Bismuth, O.; Friedman, N.; Sheves, M.; Ruhman, S. *Chem. Phys.* **2007**, *341*, 267–275.
- (25) Hou, B.; Friedman, N.; Ottolenghi, M.; Sheves, M.; Ruhman, S. *Chem. Phys. Lett.* **2003**, *381*, 549–555.
- (26) Lin, S. W.; Groesbeek, M.; van der Hoef, I.; Verdegem, P.; Lugtenburg, J.; Richard, A.; Mathies, R. A. *J. Phys. Chem. B* **1998**, *102*, 2787–2806.
- (27) Zgrablic, G.; Haacke, S.; Chergui, M. *Chem. Phys.* **2007**, *338*, 168–174.
- (28) Henry, E. R.; Hofrichter, J. *Methods Enzymol.* **1992**, *210*, 129–192.
- (29) Pfisterer, C.; Gruia, A.; Fischer, S. *J. Biol. Chem.* **2009**, *284*, 13562–13569.
- (30) Cerullo, G.; Lufer, L.; Manzoni, C.; De Silvestri, S.; Shoshana, O.; Ruhman, S. *J. Phys. Chem. A* **2003**, *107*, 8339–8344.
- (31) Garavelli, M. *Theor. Chem. Acc.* **2006**, *116*, 87–105.
- (32) Zhong, Q.; Ruhman, S.; Ottolenghi, M.; Sheves, M.; Friedman, N.; Atkinson, G. H.; Dealney, J. K. *J. Am. Chem. Soc.* **1996**, *118*, 12828–12829.
- (33) Ye, T.; Friedman, N.; Gat, Y.; Atkinson, G. H.; Sheves, M.; Ottolenghi, M.; Ruhman, S. *J. Phys. Chem. B* **1999**, *103*, 5122–5130.
- (34) Losi, A.; Wegener, A. A.; Engelhard, M.; Braslavsky, S. E. *Photochem. Photobiol.* **2001**, *74*, 495–503.

JP910853N